Fusion Engineering and Design 85 (2010) 882–889

Contents lists available at ScienceDirect

Fusion Engineering and Design

journal homepage: www.elsevier.com/locate/fusengdes

Implications of NSTX lithium results for magnetic fusion research

M. Ono[a,*], M.G. Bell[a], R.E. Bell[a], R. Kaita[a], H.W. Kugel[a], B.P. LeBlanc[a], J.M. Canik[b], S. Diem[b], S.P. Gerhardt[a], J. Hosea[a], S. Kaye[a], D. Mansfield[a], R. Maingi[b], J. Menard[a], S.F. Paul[a], R. Raman[c], S.A. Sabbagh[d], C.H. Skinner[a], V. Soukhanovskii[e], G. Taylor[a], the NSTX Research Team

[a] Princeton Plasma Physics Laboratory, PO Box 451, Princeton, NJ 08543, USA
[b] Oak Ridge National Laboratory, PO Box 2008, Oak Ridge, TN 37831, USA
[c] University of Washington at Seattle, Seattle, WA, USA
[d] Columbia University, New York, NY, USA
[e] Lawrence Livermore National Laboratory, Livermore, CA, USA

ARTICLE INFO

Article history:
Available online 8 May 2010

Keywords:
NIFS-CRC symposium
Tokamaks and spherical tokamaks
Lithium
Plasma–wall interactions

ABSTRACT

Lithium wall coating techniques have been experimentally explored on National Spherical Torus Experiment (NSTX) for the last five years. The lithium experimentation on NSTX started with a few milligrams of lithium injected into the plasma as pellets and it has evolved to a lithium evaporation system which can evaporate up to ~100 g of lithium onto the lower divertor plates between lithium re-loadings. The unique feature of the lithium research program on NSTX is that it can investigate the effects of lithium in H-mode divertor plasmas. This lithium evaporation system thus far has produced many intriguing and potentially important results; the latest of these are summarized in a companion paper by H. Kugel. In this paper, we suggest possible implications and applications of the NSTX lithium results on the magnetic fusion research which include electron and global energy confinement improvements, MHD stability enhancement at high beta, edge localized mode (ELM) control, H-mode power threshold reduction, improvements in radio frequency heating and non-inductive plasma start-up performance, innovative divertor solutions and improved operational efficiency.

1. Introduction

Various lithium wall coating techniques have been experimentally explored on a number of magnetic fusion devices for over two decades [1–5]. In experiments being conducted worldwide in varied configurations, lithium coating techniques have significantly altered and improved the plasma performance, starting with TFTR where lithium coatings produced a substantial increase in D-T fusion power in "supershot" discharges [1]. More recently, a significant energy confinement enhancement was observed in the CDX-U tokamak when recycling was reduced by a liquid lithium limiter surface [5]. In 2004, the lithium experimental research program on National Spherical Torus Experiment (NSTX) started using a few milligrams of lithium injected as pellets into the plasma. Over the intervening years, the lithium application technique has evolved to the present lithium evaporation system [6] which can deposit hundreds of milligrams of lithium onto the lower divertor plates between discharges and many tens of grams of lithium between re-loadings [6–8]. In 2009 for example, the total amount of lithium evaporated into the NSTX vessel was nearly 600 g. At present, a liquid lithium divertor plate system is being readied for plasma operation to test the effectiveness of a liquid lithium divertor surface. A unique feature of the NSTX lithium program is that it studies the effects of lithium in H-mode divertor plasmas. The NSTX lithium evaporation system thus far has produced many intriguing and potential important results; the latest of these are summarized in a companion paper by H. Kugel [9]. In this paper, we will point out the important features of the NSTX lithium evaporation results and suggest possible implications and applications to magnetic fusion research These results include electron and global energy confinement improvements, MHD stability enhancement at high beta, edge localized mode (ELM) control, H-mode power threshold reduction, improvements in radio frequency heating and non-inductive plasma start-up performance, innovative divertor solutions and improved operational efficiency. An intriguing result from NSTX is the surprisingly low levels of lithium ions measured in the NSTX H-mode plasma core (well below 1% dilution) compared to higher Z impurities (such as carbon) even when the plasma is essentially surrounded by the lithium coated walls [10]. If the lithium core dilution can be kept to a negligible level, the potential reactor applications of lithium would be greatly enhanced. For example, it may even be possible to introduce an evaporation-

* Corresponding author. Tel.: +1 609 243 2105; fax: +1 609 243 2222.
E-mail address: mono@pppl.gov (M. Ono).

0920-3796/$ – see front matter © 2010 Elsevier B.V. All rights reserved.
doi:10.1016/j.fusengdes.2010.03.045

cooling-based liquid lithium divertor chamber [11] for handling the extreme heat load expected in tokamak-based fusion demonstration power plants. Lastly, the introduction of the lithium evaporator enabled a significant improvement in the NSTX plasma operations in terms of the quality and reliability of the plasma discharges as well as an increased rate of running plasma shots, which resulted in both record plasma parameters and the total number of successful plasma shots in 2009.

2. Experimental set-up

The National Spherical Torus Experiment is a MA-class spherical torus/tokamak (ST) facility [12] which is designed to explore the low-aspect-ratio tokamak regime to $R/a = 1.35$ as shown in Fig. 1. Presently, the NSTX plasmas are heated by up to 7.5 MW of deuterium Neutral Beam Injection (NBI) and up to 4 MW of High-Harmonic Fast Wave (HHFW) heating and current drive systems. The achievement of good vacuum and surface conditions on the graphite tile plasma-facing components (PFCs) in NSTX has been crucial to the progress in its plasma performance. Even prior to the lithium evaporation, NSTX employed several PFC conditioning techniques, including 350 °C bake out of PFCs, periodic boronization, and between-shots helium glow-discharge cleaning (HeGDC), to control the impurity influxes and the hydrogenic loading of the PFCs [13]. This combination of methods both suppressed oxygen impurities and reduced the ratio of the hydrogen to deuterium concentrations to below 0.05 in plasmas with deuterium fueling.

In 2007, a lithium evaporator was installed on NSTX to explore the benefit of lithium coating of PFCs on the plasma performance [6]. In Fig. 2 the experimental set-up of the present dual lithium evaporator (LITER) system is shown. The dual evaporators are placed at the top of the device aiming the lithium vapor steam toward the lower divertor graphite tiles. They are separated 150° toroidally to complete the toroidal coverage. Shutters in front of the evaporators are designed to prevent lithium entering the plasma region both during the plasma pulse (to prevent lithium deposition on diagnostic windows while their protective shutters were open) and during any subsequent period of helium glow-discharge cleaning (to prevent the entrapment of helium in the deposited lithium layer). The LITER system can be refilled with about 100 g of lithium in about a half day.

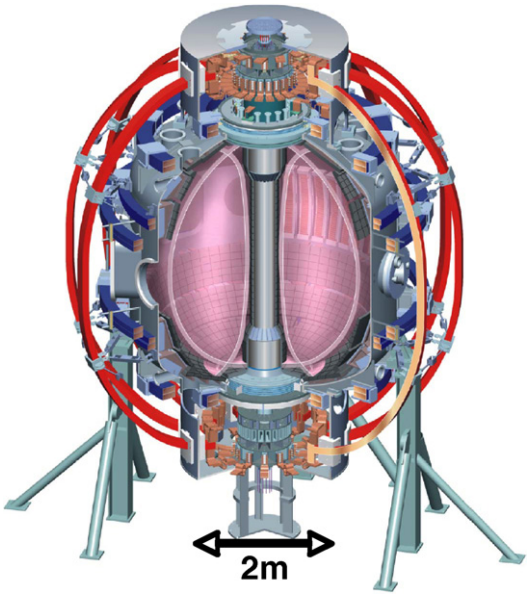

Fig. 1. A schematic of the NSTX device cross section.

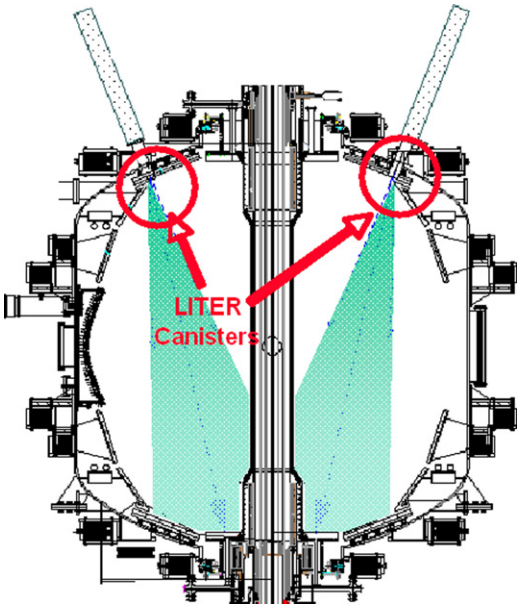

Fig. 2. A schematic of the lithium evaporators (LITERs) injecting vapor which condenses on the room-temperature plasma-facing components in the lower part of the vacuum chamber, including the lower divertor plates.

3. Improved electron energy confinement

A striking effect of the lithium evaporation on NSTX is the general improvement of plasma energy confinement where the global stored energy rises for a given heating power. In particular, the effect on the energy confinement of H-mode plasma is quite encouraging [8,9]. Kinetic measurements show that the main driver of this confinement improvement is the increase in the electron thermal stored energy which can be as much as 44% for standard H-mode discharges as shown in Fig. 3. Thomson scattering measurements show that the main improvement of the electron confinement is occurring in the outer region of the plasma making the electron temperature and thus the plasma pressure profile broader as shown in Fig. 4. TRANSP analysis confirms that electron thermal transport in outer region is progressively reduced with increasing lithium evaporation as shown in Fig. 5. The thermal ion confinement improvement is smaller since the ion confinement for the NSTX H-mode plasmas is already close to neo-classical level both with and without lithium. Previously, electron confinement improvement in NSTX was observed with increased toroidal mag-

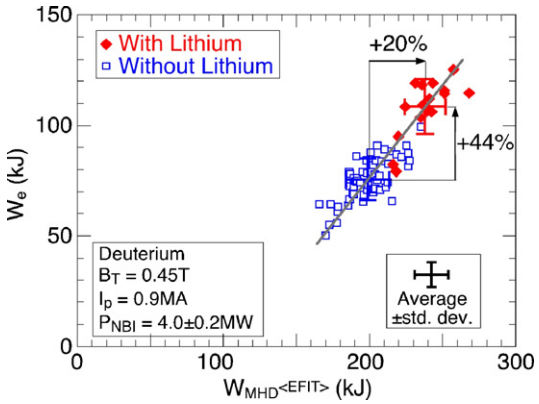

Fig. 3. Total stored energy from EFIT analysis and electron stored energy from volume integration of Thomson scattering measurements of n_e, T_e for similar H-mode discharges with and without lithium coating of the lower divertor.

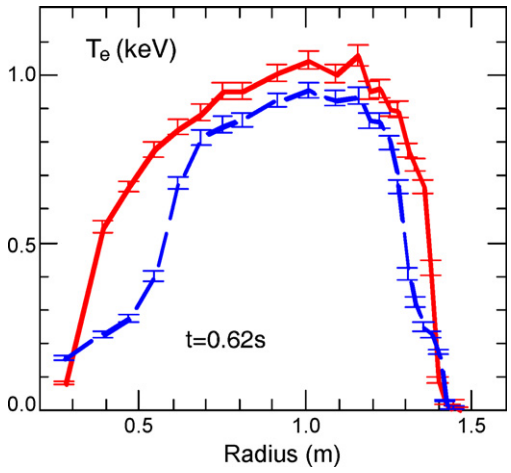

Fig. 4. Profiles of Thomson scattering measurements of electron temperature with (red) and without (blue) lithium close to the time of peak stored energy for similar H-mode discharges. (For interpretation of the references to color in this figure legend, the reader is referred to the web version of the article.)

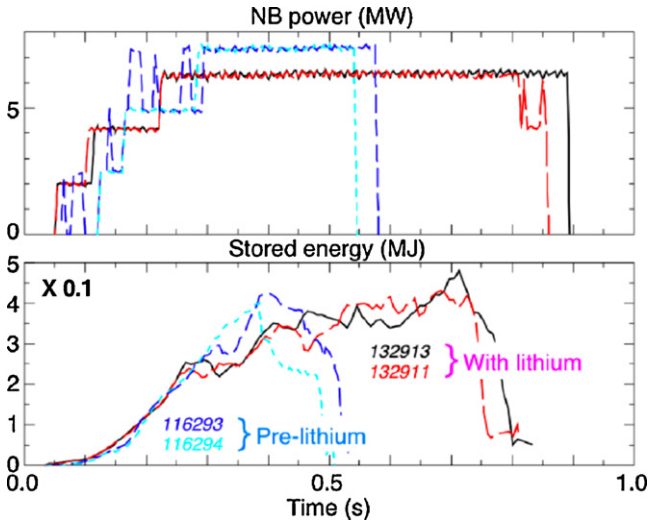

Fig. 6. High stored energy shots in NSTX. The shot 116293 produced E_p = 428 kJ with P_{NBI} = 7.5 MW at I_p = 1.4 MA. With lithium, the shot 132911 produced E_p = 480 kJ with P_{NBI} = 6 MW at I_p = 1.3 MA.

netic field [14] and with reversed shear discharges [15]. Lithium provides another (perhaps more flexible) knob to control the electron energy confinement. Another noteworthy feature of operation with lithium is that the global confinement tends to stay high even with high heating power. In Fig. 6, a comparison of high stored energy shots with and without lithium is shown. With lithium, a record stored energy of 480 kJ is achieved in a $I_p \sim 1.3$ MA plasma with 6 MW of NBI power where the global confinement time is ~80 ms. Without lithium, the highest stored energy of 428 kJ required 7.5 MW of heating power at $I_p \sim 1.4$ MA and the global confinement time of ~55 ms. As can be seen in Fig. 6, the pulse duration with lithium is also considerably longer due to the lower loop voltage. The lithium therefore helps the plasma performance by both increasing the confinement time and the pulse duration. While the mechanism of the improving electron energy confinement with lithium is not fully understood, a likely contributing factor is the lower edge recycling (as indicated by a significant drop in the H-alpha emission) produced by the lithium pumping. The application of lithium could therefore provide a relatively inexpensive way to enhance the performance of tokamak H-mode discharges including ITER. The lithium application also offers a valuable scientific tool to control the electron transport for investigating the long standing puzzle of electron energy transport. Since a burning fusion reactor plasma is heated by fusion alphas which predominantly heat electrons, the understanding and eventual control of the electron energy transport is of critical importance for magnetic fusion reactor optimization.

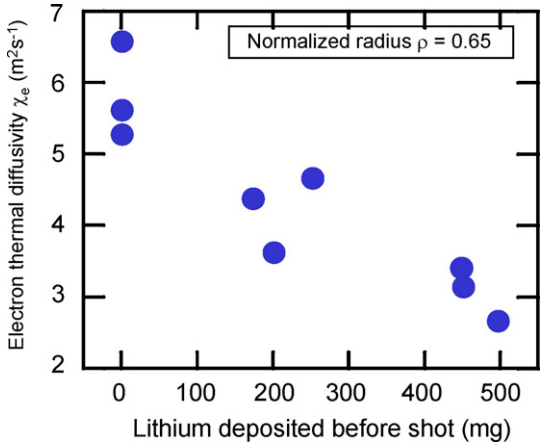

Fig. 5. Electron thermal diffusivity from TRANSP analysis in outer region of the plasma vs. lithium deposition rate.

4. Enhanced macro-stability

Tokamak plasma macro or MHD stability is the foundation for defining the tokamak reactor performance. For a given magnetic field (which represents a significant facility investment), it is desirable to maximize the plasma beta $\beta_T \equiv 2\mu_0\langle p\rangle/B_{T0}^2$ since the fusion power output is proportional to the average plasma pressure squared, i.e., $P_{fusion} \propto \langle p\rangle^2$. Tokamak plasma MHD stability is determined by various device and plasmas parameters including for example the plasma aspect ratio $A \equiv R_0/a$ where R_0 is the device major radius and a is the plasma minor radius, and the plasma elongation $\kappa \equiv (b/a)$ where b is the plasma vertical minor radius [16,17]. The plasma pressure and current profiles are two important internal plasma parameters for determining the tokamak plasma MHD stability. The MHD stability calculations predict that broader plasma pressure and current profiles are generally desirable for MHD stability at high beta which is needed for steady-state advanced tokamak operations where a large fraction of the plasma current is generated by the pressure driven bootstrap current. For example, the achievable plasma beta in NSTX for the H-mode plasmas is typically about twice that of the L-mode which has more peaked pressure and current profiles. Therefore, the H-mode is the desired mode of high beta operations for NSTX and for tokamak-based advanced reactors, in general. Additionally for a steady-state tokamak reactor, it is particularly important to achieve high $\beta_N \equiv \beta_T a B_{T0}/I_p$ since higher β_N produces a higher bootstrap current fraction $f_{BS} \propto \sqrt{\varepsilon}(1+\kappa^2)\beta_N^2/\beta_T$ [16]. In Fig. 7, the achieved β_N for the NSTX parameters is plotted as a function of plasma internal inductance $l_i \equiv \langle B_p^2\rangle/\bar{B}_p^2$ (where lower l_i indicates broader plasma current profile) [17]. As one can see from the figure, the NSTX data shows a trend of accessing higher β_N regime with lower l_i or broader current profile. For steady-state tokamak operations, the desired advanced regime, where the plasma current is largely generated through bootstrap current, is depicted by a circle in the upper left side corner of the figure (larger β_N/l_i). To access this tokamak reactor attractive regime of large β_N/l_i, l_i needs to be further reduced from the normal H-mode plasmas. A similar statement can be made for the desired broader pressure profile. In high β_N plas-

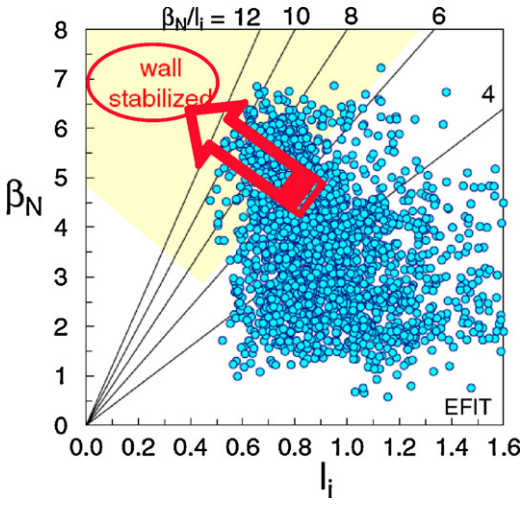

Fig. 7. NSTX MHD operational space plotted as β_N vs. l_i.

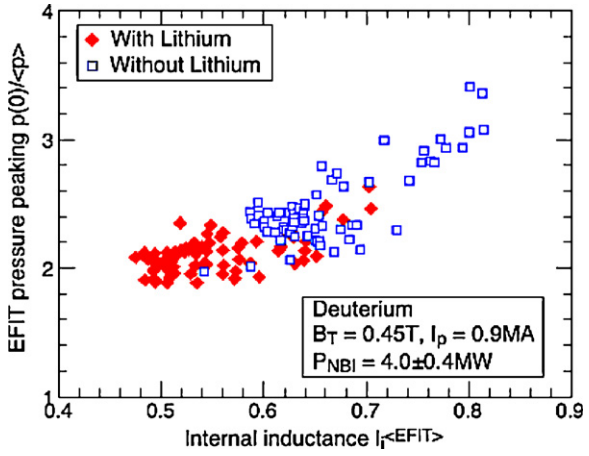

Fig. 9. Effects of lithium on MHD relevant plasma profiles. Corresponding changes in the plasma pressure peaking factor as a function of l_i.

mas, since the (pressure driven) bootstrap current fraction is quite high, the current profile and pressure profile are strongly linked. In NSTX H-mode discharges with lithium applied, a significant reduction in l_i as well as the average loop voltage was obtained, as shown in Fig. 8 [8]. The broader electron temperature profile generates a broader current profile due to the broader inductive current (owing to increased plasma conductivity in the outer region) and increase bootstrap current due to higher electron pressure and lower collisionality in the outer region. These combine to lower the loop voltage. The broader pressure profile trend with lithium is shown in Fig. 9. The broader pressure profile is largely due to the broader electron temperature profile as discussed earlier. While NSTX has not yet fully exploited the benefit of lithium induced broader pressure and current profiles on high beta MHD stability, the lithium effects of the MHD stability are generally favorable as the β_N tends to be higher and the pulse duration longer due to reduced loop voltage. The lithium is therefore a powerful tool to develop steady-state advanced tokamak operations as being pursued worldwide.

5. Edge localized modes (ELMs)

The ELMs are macroscopic instabilities in the H-mode barrier region due to the outward (unstable) forces in the outboard side (in the unfavorable curvature region). While the periodic ELMs can regulate the H-mode barrier (and the associated pressure gradient) and facilitate steady-state H-mode operation, ELMs can also cause high transient heat flux (typically an order of magnitude higher than the steady-state value) that can seriously damage the divertor plasma-facing components of future tokamak reactors including ITER. ELM stability is therefore an active high priority area of tokamak research. While ELM physics is a complex 3-D MHD phenomenon, the so-called "peeling-ballooning" model has been used with a considerable success to model the ELM stability [18]. While lithium can increase the edge electron temperature and pressure as shown in Fig. 10, the lithium evaporation in NSTX can completely stabilize ELMs. This is counter intuitive in that one would expect the increased edge pressure would destabilize the ballooning modes. However, detailed profile measurements together with edge MHD stability calculations show that ELMs can be indeed stabilized by lithium due to an inward shift of the peak pressure gradient into a region of reduced magnetic shear and somewhat wider pressure gradient width [18]. The absence of ELMs has caused improved particle confinement but also led to an accumulation in the core of high Z impurities and an eventual radiative collapse of some discharges. A technique utilizing 3-D field perturbation was developed on NSTX to induce ELMs which reduced the impurity accumulation without adversely affecting the plasma confinement improvement [19]. While the impurity radiation is a cause for concern for the

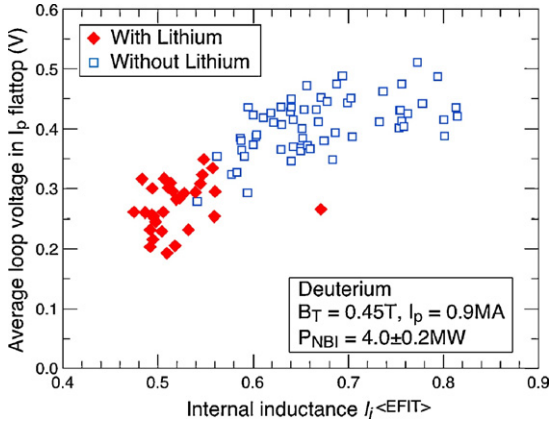

Fig. 8. Effects of lithium on MHD relevant plasma profiles. Changes of the loop voltage averaged through the plasma current flat-top and the internal inductance l_i for standard NBI-heated H-mode plasmas with and without lithium coating applied.

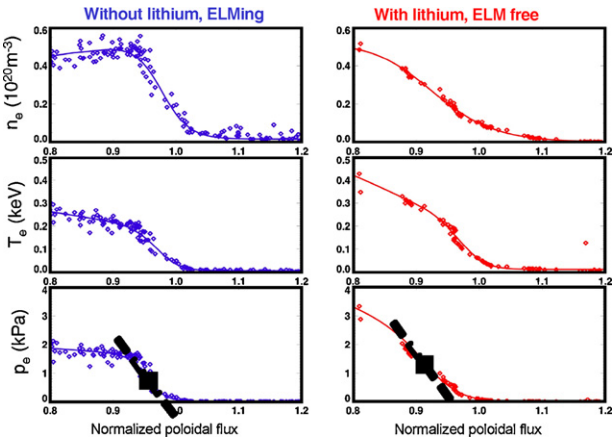

Fig. 10. Density, temperature and pressure as functions of normalized poloidal flux for two shots without (blue) and with (red) lithium. The mapped profiles are from equilibrium analysis. The data for the shot without lithium are for times within the last 20% of the ELM period. (For interpretation of the references to color in this figure legend, the reader is referred to the web version of the article.)

ELM-free discharges, the lithium's ability to influence the plasma edge pressure profile and ELMs could make it a valuable tool for future tokamak experiments including ITER.

6. H-mode power threshold

As discussed in the MHD section, the H-mode is highly desirable for high performance reactors due to its high confinement and high MHD stability at high beta. For ITER, for example, the predictive modeling shows that to achieve its high fusion gain ($Q = 10$) mission, it is essential to achieve an H-mode with sufficiently high pedestal pressure. The prediction for the heating power required to induce the H-mode (the H-mode power threshold) in ITER and future ST reactors remain uncertain since the physics of H-mode transition is not yet fully understood. Since the auxiliary heating power is expensive, it is advantageous to access the H-mode with as low heating power as possible. On NSTX, it was found that the application of lithium reduced the H-mode threshold by a factor of up to a factor of four [20]. This power threshold reduction by lithium is attributable partly to the reduced density achieved by reducing the edge recycling. However, other factors such as a lower oxygen impurity level and lower edge collisionality are also likely to be playing a role. Thus, lithium could provide a powerful tool to help future reactors such as ITER to access the H-mode regime with limited auxiliary heating power.

7. Improving HHFW/ICRH heating efficiency

The ability of lithium to reduce the edge recycling and reduce the scrape-off-layer density turned out to be highly beneficial for the High-Harmonic Fast Wave heating and current drive [21]. The plasma waves launched by an antenna must reach the main plasma region (interior of the last closed flax surface) with sufficient efficiencies to be a viable tool for reactor application. The scrape-off region, which is located between the rf antenna and the main plasma, has low plasma temperature and high neutral density (a highly dissipative region) and can be a challenging region for wave transmission that is subjected to various parasitic processes including non-linear wave-wave interactions. It should be noted that the physics of fast wave coupling is relatively insensitive to ion cyclotron harmonics ($n \equiv \omega/\Omega_i$) at the plasma edge region so the fast wave coupling physics applies well to both HHFW and ICRF heating regimes. With HHFW, the core electrons in NSTX can be heated from a few hundred eV with Ohmic heating to 6 keV range. The discharge also transitions into an H-mode in which the electron temperature significantly broadens but still retains high core temperature characteristics. The HHFW heating efficiency however depends sensitively on the plasma condition and antenna phasing. It was discovered that edge plasma density control is highly important for efficient HHFW coupling [22]. The heating efficiency is shown to depend strongly on the propagation onset density which depends on the launched wave number and toroidal magnetic field. An example is shown in Fig. 11 where the higher edge density at the beginning of the discharge results in much lower core heating efficiency. If the edge density is too high, the launched fast wave at the edge could lose the power before reaching the main plasma. An important density parameter is the wave cut-off condition given as $\omega_{pi}^2 = (\omega + \Omega_i)\Omega_i(n_{||}^2 - 1)$ where $n_{||}$ is the parallel wave index of refraction and Ω_i is the ion cyclotron frequency. The wave cut-off density can be then given as $n_e(10^9\ \mathrm{cm}^{-3}) = (5.0Z/\mu)(n+1)B_T^2(n_{||}^2 - 1)$ where Z and μ are charge and atomic mass number of working gas ions and B_T is in T. It is important to keep the edge density (in the vicinity of the antenna) to be below the cut-off density to insure that the wave propagation starts well away from the antenna close to the main plasma to avoid

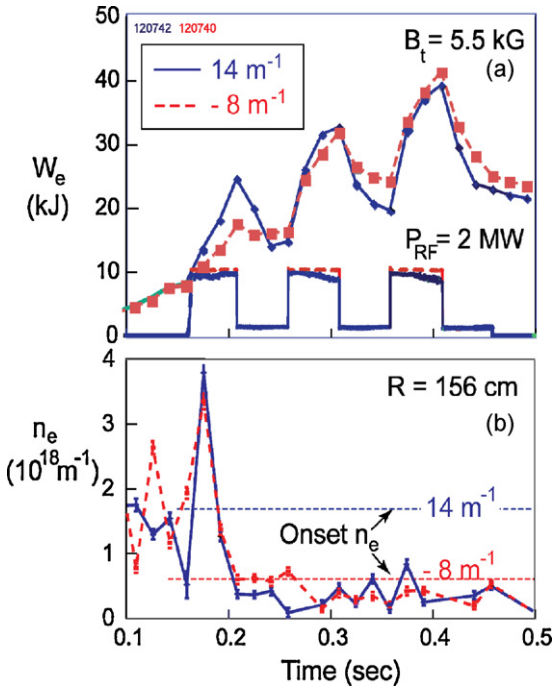

Fig. 11. (a) Electron stored energy evolution with modulated HHFW power of 2 MW with $k_\phi = 14\ \mathrm{m}^{-1}$ and $-8\ \mathrm{m}^{-1}$, respectively. (b) Edge electron density (2 cm in front of Faraday shield) vs. time. The onset density for perpendicular propagation is indicated by the horizontal dashed lines for $k_\phi = 14\ \mathrm{m}^{-1}$ and $-8\ \mathrm{m}^{-1}$ as marked.

parasitic effects including parametric instabilities and wave scattering by edge turbulence. As one can see, the critical density goes up rapidly with the parallel wave number and the magnetic field, i.e., $n_e \propto B_T^2 n_{||}^2$. For example, the critical deuterium density is only $5 \times 10^{11}\ \mathrm{cm}^{-3}$ for $n_{||} = 10$ in $B = 0.5$ T NSTX. For higher field reactor, the condition is somewhat relaxed but low $n_{||}$ condition (such as the case for the current driving phasing) can make the critical density still relatively low. For example for ITER ICRF, the critical density is relatively low $\sim 10^{12}\ \mathrm{cm}^{-3}$ for $n_{||} = 3$ (for the current drive phasing) at $B = 5$ T. By applying lithium to keep the edge scrape-off density sufficiently low, the HHFW heating efficiency and reliability have improved significantly including successful heating in the presence of NBI, which also tend to increase the edge scrape-off density in NSTX causing the loss of HHFW heating efficiency observed earlier.

8. Improving electron Bernstein wave coupling in H-mode

The electron Bernstein wave (EBW) heating is predicted to be an attractive method for driving off-axis current drive [23] in an ST. Even a modest level of off-axis current drive is projected to improve the advanced tokamak reactor performance by improving the plasma stability at high beta. The EBW is a hot plasma wave and therefore the EBW coupling will require a mode-conversion of an electromagnetic electron cyclotron wave at the so-called mode-conversion layer. For STs, due to its high plasma dielectric values, the mode-conversion occurs in the plasma edge region. Before the introduction of lithium, it was found that in the NSTX H-mode plasmas, collisional absorption near the mode-conversion layer could significantly reduce the wave accessibility to the core plasma. In Fig. 12 (a), the EBW radiometer traces are shown in H-mode with and without lithium in the scrape-off-layer is shown. With lithium, the measured EBW radiometer temperature is much closer to the core electron temperature (measured by Thomson scattering) than for the case without lithium. The EBW coupling efficiency is estimated to be ~60–70% compared to ~10%

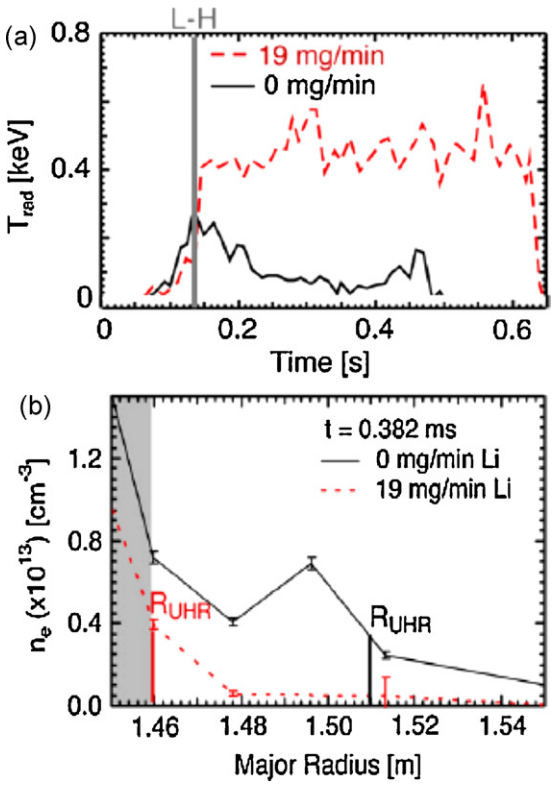

Fig. 12. (a) The EBW coupling efficiency in H-mode with and without lithium in the scrape-off-layer. (b) The Thomson scattering n_e profiles with and without lithium in the scrape-off-layer for H-mode.

without. With application of lithium, the edge plasma density as measured by the Thomson scattering [Fig. 12(b)] is indeed significantly reduced and this reduces the collisional absorption in the mode-conversion region resulting in improved EBW coupling efficiency [24].

9. Improving plasma start-up with coaxial helicity injection

The NSTX is pursuing a novel plasma start-up concept using coaxial helicity injection (CHI) [25]. While non-inductive start-up is critically needed for the low-aspect-ratio spherical tokamak due to the limited space in the in-board (high field) region, it would also provide flexibility in designing a conventional tokamak reactor as well. Fig. 13 shows a schematic drawing of the NSTX CHI system including the location of the insulating gaps between the divertor plates, the lower divertor coils used for generating the CHI injector flux and the absorber poloidal field coils. Due to a much larger applied toroidal field compared to the poloidal field, a toroidal current much larger than the electrode current (as much as 70 times in NSTX) can be generated. As the toroidal current builds up, the $J \times B$ force exceeds the so-called bubble burst condition and the toroidal current ring expands into the main chamber. In this manner, NSTX has generated the toroidal plasma current of up to 300 kA. After the applied CHI electrode voltage is turned off, the toroidal plasma current begins to form closed flux surfaces and then decays resistively. At this point, one can apply an induction voltage to further ramp up the current. Since CHI is a DC electrical discharge between electrodes, it is important to control impurity generation. With the application of lithium coating to the electrode region in a recent CHI experiment, it was possible to significantly reduce the influx of impurities (such as oxygen) and produced high quality CHI start-up tokamak discharge which actually contributed 200 kA to the inductive current generation.

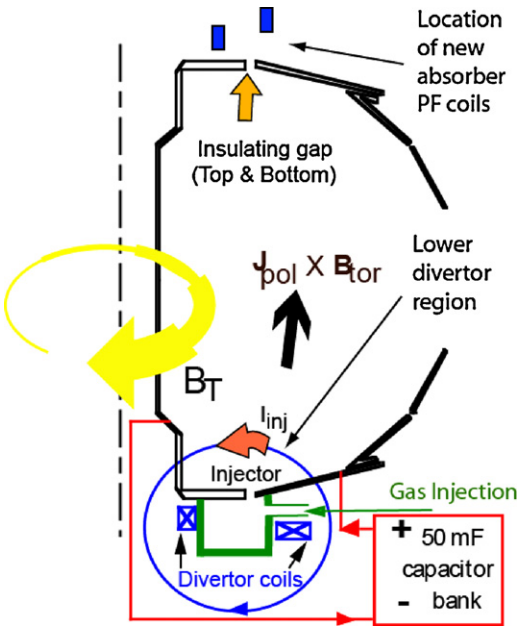

Fig. 13. NSTX CHI schematic drawing of the NSTX including the location of the insulating gaps between the divertor plates.

10. Divertor power handling

How to handle the steady-state fusion generated heat at the plasma material interface is a challenging technical issue for all toroidal magnetic fusion reactors. Since in a tokamak, the divertor plate can experience a peak time-average heat fluxes of 10–50 MW/cm^2 and even higher during the transient events such as ELMs and disruptions, it is recognized that innovative approaches to the plasma material interface are required. While experiments in NSTX were able to demonstrate a significant peak power flux reduction (5–10) by a combination of strong shaping and divertor gas injection, another order of magnitude peak heat flux reduction would likely to be needed for a reactor [26]. There are a number of innovative divertor heat flux solutions proposed recently. A "snow-flake" divertor concept which utilizes higher quality divertor field null (higher order multiple field null) can significantly enhance the divertor field expansion to reduce the divertor wall heat load [27]. A preliminary test of the snow-flake divertor was conducted on NSTX with a promising result. Another innovative concept is the super-X divertor configuration where by extending the outer divertor flux line to larger major radius, a large flux expansion is achieved that brings down the plasma temperature and creates a partially detached divertor condition. The combination of a super-X divertor together with a liquid lithium divertor surface is being examined as a promising solution for future tokamak/ST based reactors [28]. Another innovative concept for handling the steady-state divertor power is the liquid lithium divertor chamber in which lithium is continuously vaporized by the divertor heat flux [11]. Because of the large latent heat of lithium vaporization, the liquid lithium can absorb a large amount of heat which is then distributed over a larger area. A separated divertor chamber is attractive because the lithium could be largely contained within it. One crucial physics question for such liquid lithium based divertor solutions is the effect of lithium on the main plasma. If the lithium contaminates the main plasma in a significant way (such as excessive core fuel dilution which would reduce or quench the fusion reaction), then the liquid lithium base concept will not be very attractive. The measurement on NSTX however suggests an encouraging prospect for the liquid lithium based concept. Although in the NSTX experiment, lithium coating is directly applied on the graphite divertor

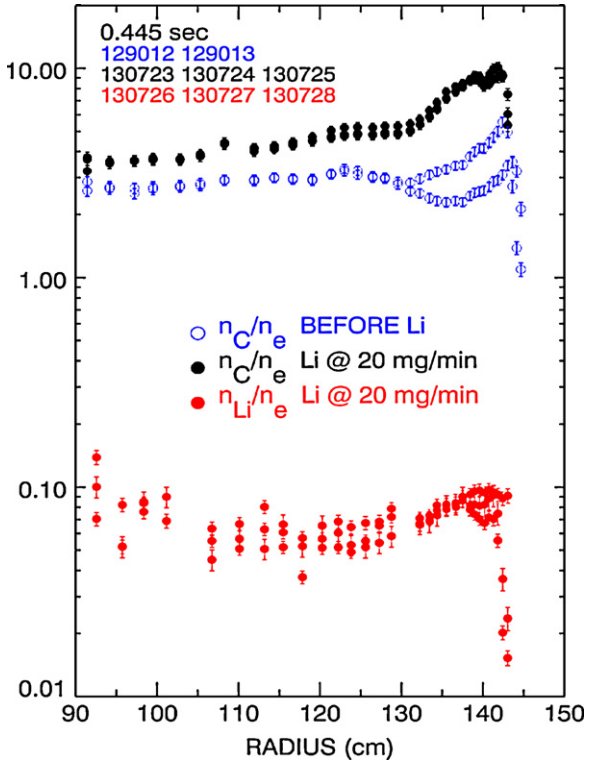

Fig. 14. Radial profiles of the lithium (red) and carbon (black, blue) for sets of similar NBI-heated, H-mode discharges. The discharges in blue were made before any lithium was applied. The discharges in black were made with ~180 mg of lithium applied section. (For interpretation of the references to color in this figure legend, the reader is referred to the web version of the article.)

plate surfaces which are in contact with the plasma, the measured lithium level in the plasma core is about 100 times lower than that of carbon as shown in Fig. 14. The low concentration of lithium compared to carbon suggests that any lithium that is injected into the plasma is rapidly ionized by the plasma due to its very low ionization potential at the outer boundary and is carried back out of the plasma before crossing the separatrix and entering the plasma core. The lithium ions tend to have a very low recycling coefficient so once escaped from the plasma, they tend to be captured by the wall. In the recent lithium aerosol experiment, for example, the NSTX discharges were remarkably tolerant of large lithium injection where the lithium ion injection rate significantly exceeded the deuterium (fueling gas) ion injection rate by as much as a factor of 5 [29]. Also, in a calculation of neo-classical transport, the light lithium ions were found to be less likely to accumulate in the plasma core compared to higher Z impurities due to the neo-classical collisional diffusion. In the case of the liquid lithium divertor chamber, the lithium vapor generated in the chamber (due to its low mass) is likely to be swept back into the divertor chamber by the impinging plasma flow from the main chamber. Even if the lithium vapor manages to escape into the main chamber (as in the case of NSTX), lithium will be quickly ionized and the likelihood of entering the plasma core appeared to be very small. The NSTX observation together with the theoretical expectations of lithium ion transport therefore suggests that the introduction of significant amount of lithium into the fusion environment may be relatively benign for the reactor performance.

11. Improved operations

The introduction of lithium evaporator on NSTX has produced a significant benefit for the NSTX operations. As can be seen in Table 1, the NSTX operational efficiency given as the number of successful plasma shots per one run week has steadily improved since the introduction of lithium evaporator in 2007. In 2009, the fractional lithium operation has increased to over 90% which contributed to the record number of shots per week as well as the total number of shots obtained in one year. The lithium evaporation not only maintains a lower oxygen impurity level but it also controls the level of hydrogenic gas wall retention to enable reproducible plasma shots without applying helium glow discharges (HeGDC) between plasma shots. Before lithium was routinely used, HeGDC was performed typically for about 10 min between high power discharges which limited the number of plasma shots to about 3 per hour. With lithium, the number of plasma shots can be increased to the usual machine operating cycle of about 4 per hour limited by cooling of the coils and time for data analysis. The lithium application also tends to produce more MHD quiescent plasmas which further improves the plasma operational reliability. The lithium clean up process performed during the maintenance period is described in the companion paper by Kugel et al. [9] at this conference.

Table 1
NSTX plasma operations statistics for 2004–2009. The lithium evaporator was used after 2007 and its utilization reached over 90% in 2009.

NSTX plasma operations statistics				
Year	Weeks	Shots	Shots/week	Lithium %
2009	16.84	2750	163	92
2008	16.5	2570	156	46
2007	12.6	1890	150	69
2006	12.7	1615	127	0
2005	17.97	2221	124	0
2004	21.1	2460	117	0

12. Conclusions

The lithium evaporation on the lower divertor region in NSTX has yielded a number of important benefits to the NSTX research in terms of intriguing science results and operational improvements. The improved electron confinement in outer region has a number of potential applications such as increasing the overall plasma performance as well as improving the plasma MHD stability, and the control or mitigation of ELMs. The low recycling condition by lithium also reduced the H-mode power threshold which could benefit future reactors including ITER. The ability of lithium to reduce edge collisionality and oxygen impurity level improved the HHFW (ICRF) core heating efficiency, the EBW plasma coupling, and the CHI non-inductive start-up. The NSTX H-mode plasma shows a surprisingly small amount of core contamination by lithium with less than 1% deuterium fuel dilution by lithium. This observation bodes well for those concepts which introduce significant quantity of lithium into the vacuum chamber such as the liquid lithium evaporation based divertor chamber for steady-state divertor heat flux handling [11]. Operationally, lithium conditioning has improved the NSTX plasma performance in terms of record plasma stored energy and lower loop voltage. It has also resulted in more reliable plasma operation with about 30% increase in the number of plasma shots achieved per week. Overall, the lithium has a very exciting prospect in contributing to the magnetic fusion research as a powerful tool to control the plasma edge and as a potential solution for the very challenging fusion tokamak/ST reactor divertor heat flux problem.

Acknowledgement

This work was supported by DoE Contract No. DE-AC02-09CH11466.

References

[1] D.K. Mansfield, D.W. Johnson, B. Grek, H.W. Kugel, M.G. Bell, R.E. Bell, et al., Nucl. Fusion 41 (2001) 1823.
[2] S.V. Mirnov, V.B. Lazarev, S.M. Sotnikov, V.A. Evtikhin, I.E. Lyublinski, A.V. Verkov, T-11M Team Fusion Eng. Des. 65 (2003) 455–465.
[3] M.L. Apicella, et al., J. Nucl. Mater. 363–365 (2007) 1346–1351.
[4] J. Sanchez, F.L. Tabares, D. Tafalla, J.A. Ferreira, I. Garcia-Cortes, C. Hidalgo, et al., J. Nucl. Mater. 390–391 (2009) 852–857.
[5] R. Majeski, R. Doerner, T. Gray, R. Kaita, R. Maingi, D. Mansfield, et al., Phys. Rev. Lett. 97 (2006) 075002.
[6] H.W. Kugel, M.G. Bell, J.-W. Ahn, J.P. Allain, R. Bell, J. Boedo, et al., Phys. Plasmas 15 (2008) 056118.
[7] D.K. Mansfield, H.W. Kugel, R. Maingi, M.G. Bell, R. Bell, R. Kaita, et al., J. Nucl. Mater. 390–391 (2009) 764–767.
[8] G. Michael, H.W. Bell, R. Kugel, L.E. Kaita, H. Zakharov, Schneider, et al., Plasma Phys. Controlled Fusion 51 (2009) 124054.
[9] H. Kugel, M.G. Bell, H. Schneider, J.P. Allain, R. E. Bell, R. Kaita, et al., Fusion Eng. Des., accepted for publication, 2010.
[10] R. Bell, Private Communication.
[11] Y. Nagayama, Fusion Eng. Des. 84 (2009) 1380.
[12] M. Ono, S.M. Kaye, Y.-K.M. Peng, G. Barnes, W. Blanchard, M.D. Carter, et al., Nucl. Fusion 40 (2000) 557.
[13] H.W. Kugel, R. Maingi, W. Wampler, R.E. Barry, M. Bell, W. Blanchard, et al., J. Nucl. Mater. 290 (2001) 1185.
[14] S.M. Kaye, R.E. Bell, D. Gates, B.P. LeBlanc, F.M. Levinton, J.E. Menard, et al., Phys. Rev. Lett. 98 (2007) 1175002.
[15] F.M. Levinton, H. Yuh, M.G. Bell, R.E. Bell, D. Delgado-Aparicio, M. Finkenthal, et al., Phys. Plasmas 14 (2007) 056119.
[16] J.E. Menard, M.G. Bell, R.E. Bell, D.A. Gates, S.M. Kaye, B.P. LeBlanc, et al., Phys. Plasmas 11 (2004) 639.
[17] S.A. Sabbagh, A.C. Sontag, J.M. Bialek, D.A. Gates, A.H. Glasser, J.E. Menard, et al., Nucl. Fusion 46 (2006) 635.
[18] R. Maingi, T.H. Osborne, B.P. LeBlanc, R.E. Bell, J. Manickam, P.B. Snyder, et al., Phys. Rev. Lett. 103 (2009) 075001.
[19] J.M. Canik, R. Maingi, T.E. Evanc, R.E. Bell, S.P. Gerhardt, B.P. LeBlanc, et al., Phys. Rev. Lett. 104 (2010) 045001.
[20] S. Kaye, Private Communication.
[21] M. Ono, Phys. Plasmas 2 (1995) 4075.
[22] J. Hosea, R.E. Bell, B.P. LeBlanc, C.K. Phillips, G. Taylor, E. Valeo, et al., Phys. Plasmas 15 (2008) 056104.
[23] G. Taylor, P.C. Efthimion, C.E. Kessel, R.W. Harvey, A.P. Smironv, N.M. Ershov, et al., Phys. Plasmas 11 (2004) 4733.
[24] S.J. Diem, G. Taylor, J.B. Caughman, P.C. Efthimion, H. Kugel, B.P. LeBlanc, et al., Nucl. Fusion 49 (2009) 095027.
[25] R. Raman, T.R. Jarboe, D. Mueller, B.A. Nelson, M.G. Bell, R. Bell, et al., Nucl. Fusion 49 (2009) 065006.
[26] V.A. Soukhanovskii, R. Maingi, D.A. Gates, J.E. Menard, S.F. Paul, R. Raman, et al., Nucl. Fusion 49 (2009) 095025.
[27] D.D. Ryutov, Phys. Plasmas 14 (2007) 064502.
[28] P.M. Valanju, M. Kotschenreuther, S.M. Mahajan, J. Canik, Phys. Plasmas 16 (2009) 056110.
[29] D.K. Mansfield, A.L. Roquemore, H. Schneider, J. Timberlake, H. Kugel, M. Bell, et al., Fusion Eng. Des., submitted 2010.